

Gerasco Joy (Orcid ID: 0000-0002-5074-4281)
Hatch Nan E (Orcid ID: 0000-0002-2632-0841)
Novince Chad Michael (Orcid ID: 0000-0002-0318-7494)

Commensal Microbiota Effects on Craniofacial Skeletal Growth and Morphology

Joy E. Gerasco, D.M.D., Ph.D.^{1,2,3,4} (joyeg@ad.unc.edu), Jessica D. Hathaway-Schrader, Ph.D.^{1,2,3} (hathawa@musc.edu), Nicole A. Poulides, M.S.^{1,2,3} (nicole.poulides@utsouthwestern.edu), Matthew D. Carson^{1,2,3} (carsonma@musc.edu), Naoto Okhura, D.D.S., Ph.D.⁵ (naotoo@umich.edu), Caroline Westwater, Ph.D.^{1,6} (westwatc@musc.edu), Nan E. Hatch, D.M.D., Ph.D.⁵ (nhatch@umich.edu), Chad M. Novince, D.D.S., M.S.D., Ph.D.^{1,2,3} (novincec@musc.edu)

¹Department of Oral Health Sciences, College of Dental Medicine, Medical University of South Carolina, Charleston, SC, USA; ²Department of Stomatology-Division of Periodontics, College of Dental Medicine, Medical University of South Carolina, Charleston, SC, USA; ³Department of Pediatrics-Division of Endocrinology, College of Medicine, Medical University of South Carolina, Charleston, SC, USA; ⁴Department of Orthodontics, Adam's School of Dentistry, University of North Carolina, Chapel Hill, NC, USA; ⁵Department of Orthodontics and Pediatric Dentistry, School of Dentistry, University of Michigan, Ann Arbor, MI, USA; ⁶Department of Microbiology and Immunology, College of Medicine, Medical University of South Carolina, Charleston, SC, USA.

Running title: Microbiota Effects Craniofacial Skeletal Morphology

Conflicts of Interest: None.

Funding: American Society for Bone and Mineral Research Rising Star Award, K08DE025337, T32DE017551, P20GM130457, P30DK123704, P20GM121342, R01DE029637, R01AG067510, UL1TR001450, F30DE027290

Study approval. Animal research was approved by the MUSC Institutional Animal Care and Use Committee and was performed in accordance with approved guidelines.

Corresponding author: Chad M. Novince, D.D.S., M.S.D., Ph.D., Department of Oral Health Sciences, Medical University of South Carolina, 173 Ashley Avenue, Charleston, SC 29425, USA Tel: +1-843-792-4957; fax: +1-843-792-6626; E-mail: novincec@musc.edu

Data availability: The data used and/or analyzed during the current study are available from the corresponding author upon request.

This is the author manuscript accepted for publication and has undergone full peer review but has not been through the copyediting, typesetting, pagination and proofreading process, which may lead to differences between this version and the Version of Record. Please cite this article as doi: [10.1002/jbm4.10775](https://doi.org/10.1002/jbm4.10775)

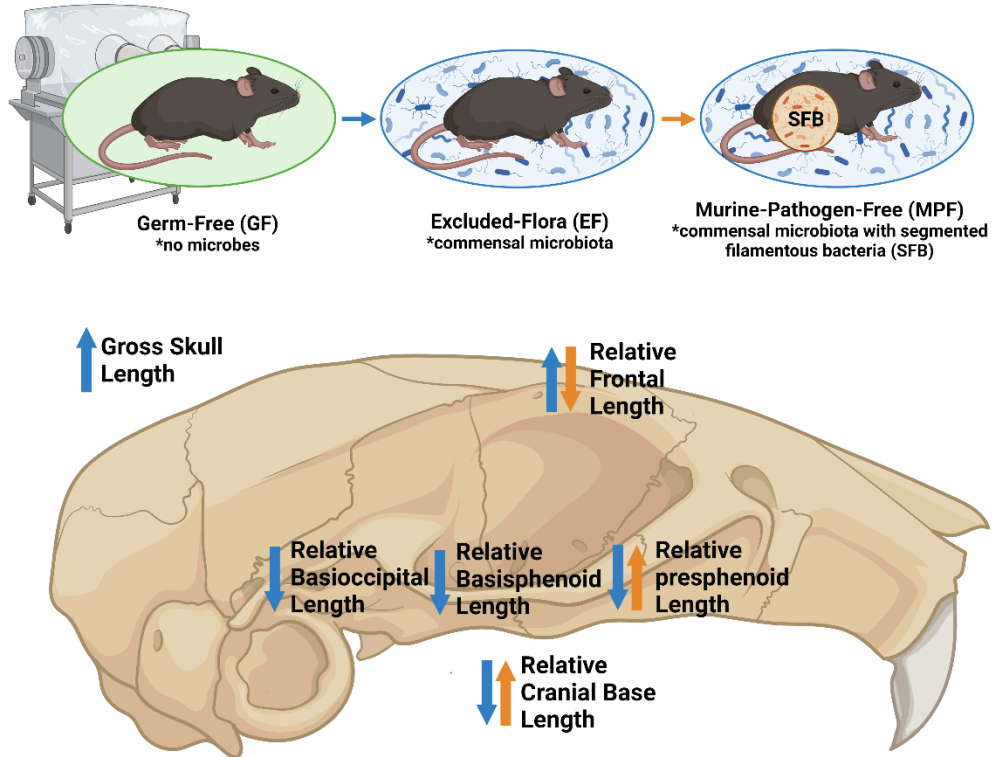
This article is protected by copyright. All rights reserved.

Abstract:

Microbes colonize anatomical sites in health to form commensal microbial communities (e.g., commensal gut microbiota, commensal skin microbiota, commensal oral microbiota). Commensal microbiota has indirect effects on host growth and maturation through interactions with the host immune system. The commensal microbiota was recently introduced as a novel regulator of skeletal growth and morphology at non-craniofacial sites. Further, we and others have shown that commensal gut microbes, such as segmented filamentous bacteria (SFB), contribute to non-craniofacial skeletal growth and maturation. However, commensal microbiota effects on craniofacial skeletal growth and morphology are unclear. To discern the commensal microbiota's role in craniofacial skeletal growth and morphology, we performed craniometric and bone mineral density analyses on skulls from 9-week-old female C57BL/6T germ-free (GF) mice (no microbes), excluded-flora (EF) specific-pathogen-free mice (commensal microbiota), and murine-pathogen-free (MPF) specific-pathogen-free mice (commensal microbiota with SFB). Investigations comparing EF mice and GF mice revealed that the commensal microbiota impacts the size and shape of the craniofacial skeleton. EF vs. GF mice exhibited an elongated gross skull length. Cranial bone length analyses normalized to skull length showed that EF vs. GF mice had enhanced frontal bone length and reduced cranial base length. The shortened cranial base in EF mice was attributed to decreased presphenoid, basisphenoid, and basioccipital bone lengths. Investigations comparing MPF mice and EF mice demonstrated that commensal gut microbes play a role in craniofacial skeletal morphology. Cranial bone length analyses normalized to skull length showed that MPF vs. EF mice had reduced frontal bone length and increased cranial base length. The elongated cranial base in MPF mice was due to enhanced presphenoid bone length. This work introducing the commensal microbiota as a contributor to craniofacial skeletal growth, underscores that non-invasive interventions in the gut microbiome could potentially be employed to modify craniofacial skeletal morphology.

Key Words: PRECLINICAL STUDIES, BONE-MICROBIOTA INTERACTORS, CRANIOMETRY

Commensal Microbiota Contributions to Craniofacial Skeletal Morphology



Graphical Abstract Description: Comparing germ-free mice (no microbes) to excluded-flora mice (commensal microbiota), showed the commensal microbiota influences craniofacial skeletal growth and morphology (*blue arrows denote commensal microbiota-induced changes). Comparing excluded-flora mice (commensal microbiota) to murine-pathogen-free mice (commensal microbiota with segmented filamentous bacteria; SFB), revealed that specific commensal gut microbes contribute to craniofacial skeletal growth and morphology (*orange arrows denote SFB-induced changes).

Introduction:

Non-pathogenic microbes colonize host anatomic barrier sites to form commensal microbiota communities (e.g., commensal gut microbiota, commensal skin microbiota, commensal oral microbiota).¹⁻⁴ Commensal microbiota interactions with the host directs the development of immunity, which has indirect effects on host growth and maturation.⁵⁻⁸ The commensal microbiota was recently introduced as a critical regulator of skeletal growth and morphology at non-craniofacial sites.⁹⁻¹⁴ Moreover, our group and others have shown that commensal gut microbes, such as segmented filamentous bacteria (SFB), contribute to non-craniofacial skeletal growth and maturation.^{13,14}

The craniofacial skeleton is a unique skeletal complex that derives from the neural crest and mesoderm and develops through both intramembranous and endochondral ossification.^{15,16} The craniofacial skeleton houses the brain and sensory organs for vision, hearing, taste, and smell, supports mastication and speaking, and impacts appearance and psychosocial well-being. Therefore, mechanisms regulating craniofacial growth and morphology are of importance.^{17,18} Murine models have been extensively used to study normal craniofacial development¹⁹⁻²¹ and craniofacial malformations caused by genetics, teratogens, and environmental factors.²²⁻²⁴ However, the role of the commensal microbiota in physiologic craniofacial skeletal growth and morphology is unknown.

To define the commensal microbiota's role in normal craniofacial skeletal growth and morphology, we performed studies comparing germ-free (GF) mice, excluded-flora (EF) mice, and murine-pathogen-free (MPF) mice. GF mice, which are devoid of all microbes, are reared in sterile isolators. Specific-pathogen-free mice, which are colonized by commensal microbiota, are reared in ventilated isolators within barrier facilities that validate specific microbes are not present. Taconic Biosciences animal health barrier facilities provided the opportunity to acquire specific-pathogen-free mice that differ by the known colonization status of SFB. EF mice are specific-pathogen-free mice that are devoid of SFB and MPF mice are specific-pathogen-free mice that harbor SFB. SFB is a commensal gut bacterium that colonizes the ileum following weaning.²⁵⁻²⁷ SFB colonization critically influences commensal microbiota actions on host immunity and development.^{13,14,27-30} Therefore,

comparing specific-pathogen-free mice that differ by SFB colonization status provides insight about the role of commensal gut microbes in commensal microbiota effects on normal growth and morphology.

Cephalometric and craniometric measurements are used in surgical and dentofacial orthopedic treatment planning to treat craniofacial malformations and achieve a more harmonious dentofacial complex.^{31,32} Craniometry is utilized in pre-clinical murine model research to advance knowledge about abnormal and healthy craniofacial skeletal growth and development¹⁹⁻²⁴. Herein, we performed craniometric and bone mineral density analyses in skulls from 9-week-old female C57BL/6T GF mice (no microbes), EF mice (commensal microbiota), and MPF mice (commensal microbiota with SFB). Comparing GF mice to EF mice, facilitated defining the role of the commensal microbiota in normal craniofacial skeletal growth and morphology. Comparing EF mice to MPF mice, supported discerning commensal gut microbe contributions to physiologic craniofacial skeletal growth and morphology.

Materials and Methods:

Mice

C57BL/6T GF mice were obtained from Taconic Biosciences (Rensselaer, NY, USA), and were bred and maintained in sterile isolators at the Medical University of South Carolina (MUSC; Charleston, SC, USA) Gnotobiotic Animal Core. GF mice were fed autoclaved LabDiet 5010 (LabDiet, St. Louis, MO, USA). Nine-week-old EF mice and MPF mice were obtained from Taconic Biosciences (Rensselaer, NY, USA), where they were bred and maintained in their respective barrier facilities. EF and MPF mice were fed autoclaved NIH-31M diet (Envigo, Indianapolis, IN, USA). Upon arrival to MUSC, EF and MPF were housed in a specific-pathogen-free vivarium and sacrificed within 48 hours. All animals were euthanized at 9.0 - 9.5 weeks of age. Animals were group housed 4-5 per cage. Room temperature and humidity were maintained within the recommended ranges advised by the *Guide for the Care and Use of Laboratory Animals*.³³ Room light:dark cycle was maintained

on a 12 hour on:off schedule. Animal experimentation was approved by the MUSC Institutional Animal Care and Use Committee and carried out in accordance with approved guidelines.

Quantitative Real-Time PCR (qRT-PCR) 16S rDNA Analyses

Following euthanasia, ileum contents were collected for bacterial 16S rDNA analysis. Genomic DNA was isolated using Qiagen DNeasy Powersoil Pro Kit (Qiagen, Hilden, Germany), per the manufacturer's instructions.

Total DNA was quantified using the Nanodrop 1000 (Thermo Scientific; Waltham, MA, USA). 16S rDNA was amplified on the StepOnePlus System (Applied Biosystems; Foster City, CA, USA) via a qRT-PCR reaction protocol using 2X Fast SYBR Green Master Mix (Applied Biosystems) forward/reverse primers (Integrated DNA Technology; Coralville, IA, USA), and DNA template, as described previously³⁴⁻³⁶. A 30-cycle qRT-PCR protocol was utilized; cycle number 25 was the cutoff for non-specific amplification of the Universal 16S gene^{13,37}. *Bacterial load analysis*: Bacterial load was evaluated by normalizing the Universal 16S gene to a

bacterial DNA standard (ZymoBIOMICS; Zymo Research, Irvine, CA, USA), as described previously^{13,36,38}.

Relative quantification of Universal 16S rDNA was carried out by the $2^{-\Delta CT}$ method³⁹. *Bacterial phyla analysis*:

Phylum level outcomes are reported relative to the Universal 16S gene, as described previously^{36,38}. Relative

quantification of phylum-level rDNA was performed by the $2^{-\Delta\Delta CT}$ method⁴⁰. *SFB analysis*: SFB presence was

evaluated by normalizing the SFB rDNA gene to a bacterial DNA standard (ZymoBIOMICS; Zymo Research),

as described previously^{13,41}. Relative quantification of SFB rDNA was performed by the $2^{-\Delta CT}$ method³⁹.

Integrated DNA Technologies forward (F) / reverse (R) primer sequences included:

Universal 16S³⁴: F=5'-AAACTCAAAGGAATTGACGG-3'; R=5'-CTCACRRCACGAGCTGAC-3'.

Pseudomonadota³⁴: F=5'-TCGTCAGCTCGTGTGTGA-3'; R=5'-CGTAAGGGCCATGATG-3'.

Actinomycetota³⁴: F=5'-TACGGCCGCAAGGCTA-3'; R=5'-TCRTCCCCACCTTCCTCCG-3'.

Bacteroidota³⁴: F=5'-CRAACAGGATTAGATACCCT-3'; R=5'-GGTAAGGTTTCCTCGCGTAT-3'.

Bacillota³⁴: F=5'-TGAAACTYAAAGGAATTGACG-3'; R=5'-ACCATGCACCACCTGTC-3'.

SFB^{13,41}: F=5'-GACGCTGAGGCATGAGAGCAT-3'; R=5'-GACGGCACGGATTGTTATTCA-3'.

Quantitative Real-Time PCR (qRT-PCR) mRNA Analyses

Ileum specimens were flash-frozen, pulverized, and homogenized in TRIzol Reagent (Invitrogen; Carlsbad, CA, USA). RNA extraction was performed via the TRIzol method, as reported previously^{13,41}. Total RNA was quantified via the NanoDrop 1000 (Thermo Scientific). cDNA was synthesized from RNA using Taqman Random Hexamers and Reverse Transcription Reagents (Applied Biosystems), following the manufacturer's protocol.^{13,41} mRNA was amplified on the StepOnePlus System (Applied Biosystems) via a qRT-PCR reaction protocol using TaqMan Fast Advanced Master Mix and primer-probes (Applied Biosystems), as described previously.^{13,41} Relative quantification of mRNA was performed by the $2^{-\Delta\Delta CT}$ method⁴⁰; *Gapdh* was used as an internal control gene. TaqMan primer-probe assays used included: *Gapdh* = Mm99999915_g1; *Ill17a* = Mm00439618_m1.

Tibia Micro-Radiograph Imaging / Length Analysis

Following euthanasia, tibiae were isolated and fixed in 10% phosphate-buffered formalin for 24 hours at room temperature; specimens were stored in 70% ethanol at 4°C. Ex vivo micro-radiographs of tibiae were acquired with a Faxitron LX-60 (Faxitron X-ray, Lincolnshire, IL, USA), using the following acquisition parameters: beam energy = 36 kVp, exposure time = 40 seconds. Tibia length measurements were performed via calibrated micro-radiograph images, measuring from the intercondylar eminence to the lateral malleolus.

Skull Micro-CT Imaging

Following euthanasia, skulls were isolated and fixed in 10% phosphate-buffered formalin for 24 hours at room temperature; specimens were stored in 70% ethanol at 4°C. Mandibles were dissected and skull specimens were scanned with a Scanco Medical μ CT 40 scanner (Scanco Medical; Brüttisellen, Switzerland), using the following acquisition parameters: X-ray tube potential = 70 kVp, X-ray intensity = 55 μ A, integration time = 200 ms, and isotropic voxel size = 18 μ m³. Calibrated 3-dimensional images of skulls were reconstructed for craniometric measurements and bone mineral density analyses.

Micro-CT Craniometric Analyses

Skull craniometric measurements were performed using Analyze 14.0 Bone Microarchitecture Analysis software (Analyze Direct; Seattle, WA, USA). Linear measurements were carried out on reoriented 3-dimensional micro-CT reconstructions, with a fixed threshold of 2500 Hounsfield units (HU). For frontal and parietal bones, linear measurements were taken bilaterally and averaged. Linear measurements were performed three separate times for each outcome of interest, and the arithmetic mean of these measurements is reported for each biological replicate. Skull length (nasale to pario) is reported as a direct measurement. All other linear measurements were normalized to skull length (nasale to pario) to account for skull size differences, as reported previously.⁴²⁻⁴⁴ Landmarks for craniometric analyses are depicted via schematics: skull length, skull width, and skull height (**Supplemental Fig. S1A**); skull length, nasal bone length, cranial vault bone lengths, and cranial base bone lengths (**Fig. 2A**). Studies were performed and are reported in accordance with guidelines for assessment of bone microstructure in rodents using micro-CT.⁴⁵

Micro-CT Bone Mineral Density Analyses

Skull bone mineral density measurements were acquired using Analyze 14.0 Bone Microarchitecture Analysis software (Analyze Direct). Bone mineral density analyses were carried out using reoriented 3-dimensional micro-CT reconstructions. A fixed threshold of 2000 HU was used to discern mineralized tissue. Bone mineral density analysis was performed in the following volumes of interest, adapted from methods described previously:^{21,46,47}
Basioccipital bone analysis: 900 μm^3 volume of interest (VOI) positioned 180 μm posterior to the junction of the basisphenoid and basioccipital bones, the spheno-occipital synchondrosis (SOS). The VOI was centered medio-laterally across the median sagittal plane. *Basisphenoid bone analysis:* 900 μm^3 VOI positioned 360 μm anterior to the SOS and 360 μm superior from the inferior extent of the pterygoid bone/process at the intersection of the SOS. *Presphenoid bone analysis:* 900 μm^3 VOI positioned 270 μm anterior to the junction of the basisphenoid and presphenoid bones, the intersphenoid synchondrosis (ISS). The VOI was oriented in the superior-inferior and

medio-lateral directions centered on the presphenoid bone. *Frontal bone analysis*: 1440 μm^3 VOI was analyzed at the left frontal bone. The VOI was positioned 720 μm lateral to the sagittal suture and 1440 μm anterior to the coronal suture. *Parietal bone analysis*: 1440 μm^3 VOI was analyzed at the left parietal bone. The VOI was positioned 1440 μm lateral to the sagittal suture and centered between the lambdoid and coronal sutures in the anterior-posterior plane. *Interparietal bone analysis*: 900 μm^3 VOI positioned 900 μm anterior to the junction of the interparietal and occipital bones. The VOI was centered medio-laterally across the median sagittal plane. Landmarks and VOIs for BMD analysis are depicted via schematics: cranial vault bones (**Supplemental Fig. S2A**); cranial base bones (**Supplemental Fig. S2E**). Studies were performed and are reported in accordance with guidelines for assessment of bone microstructure in rodents using micro-CT.⁴⁵

Statistical analysis

Statistical analysis was carried out using GraphPad Prism 9.0 (GraphPad; La Jolla, CA, USA). Unpaired two-tailed t-test (P-value < 0.05) was performed comparing 16S rDNA analysis outcomes in EF vs. MPF mice. One-way ANOVA (alpha = 0.05) with Tukey post-hoc test (P-value < 0.05) was carried out comparing outcomes in GF, EF, and MPF mice for all other studies. When unpaired t test was used, F test was performed to validate the data come from populations that are Gaussian and have equal variances. When one-way ANOVA was utilized, Brown-Forsythe test and Levene test was carried out to validate the data come from populations that are Gaussian and have equal variances. The Shapiro-Wilk test (alpha = 0.05) was applied to all data sets to determine whether the data come from normally distributed populations. In the case that the Shapiro-Wilk test did not validate that a data set was normally distributed, the ROUT outlier test (Q = 0.1%) was performed to remove definitive outliers. Data is plotted as box and whisker plots that display all data points, the interquartile range (height of the box), median (internal horizontal bar), arithmetic mean (“plus” sign), and maximum and minimum values (external upper and lower bars). Power analysis was performed based on the authors’ prior experience investigating skeletal morphology in mice, and was carried out in consultation with the MUSC Bioinformatics Core Biostatistical Unit.

Results:

The commensal microbiota does not alter somatic growth in 9-week-old female C57BL/6T mice.

We compared 9-week-old female C57BL/6T GF mice (no microbes) and EF mice (commensal microbiota), to determine the commensal microbiota's role in craniofacial skeletal growth and morphology (**Fig. 1A**). We compared 9-week-old female C57BL/6T EF mice (commensal microbiota) and MPF mice (commensal microbiota with SFB), to delineate whether commensal gut microbes contribute to commensal microbiota effects on craniofacial skeletal growth and morphology (**Fig. 1A**).

16S rDNA analyses were performed with ileum contents to validate the murine gut microbiome phenotype (**Fig. 1B-D**). Bacteria were not detectable in GF mice (**Fig. 1B-D**). The bacterial load was similar (**Fig. 1B**) and bacterial phyla expression were not different (**Fig. 1C**) in EF vs. MPF mice. SFB was detected in MPF mice, but not EF mice (**Fig. 1D**). Consistent with the presence of SFB, which induces $T_H17/IL17A$ immunity^{27,28}, *Il17a* mRNA was greater than 50X higher in the ileum of MPF vs. EF mice (**Fig. 1E**).

We evaluated alterations in bodyweight and tibia length to determine commensal microbiota effects on somatic (body) growth outcomes. Bodyweight measurements were performed immediately prior to euthanasia. Tibia length measurements were carried out on ex vivo micro-radiographs of tibiae. Body weight was similar (**Fig. 1F**) and tibia length was not different (**Fig. 1G**) in GF vs. EF mice or EF vs MPF mice. These data support that the commensal microbiota does not alter somatic growth outcomes in 9-week-old female C57BL6/T mice.

The commensal microbiota impacts craniofacial skeletal morphology in 9-week-old female C57BL/6T mice.

We performed craniometric measurements on reconstructed 3-dimensional micro-CT images of skulls to evaluate commensal microbiota effects on craniofacial skeletal growth and morphology (**Fig. 2, Supplemental Fig. S1**). Skull length (**Fig. 2A**) is reported as a direct measurement. Skull width (**Fig. 2B**), skull height (**Fig. 2C**), nasal bone length (**Fig. 2D**), cranial vault bone lengths (**Fig. 2E-H**), and cranial base bone lengths (**Fig. 2I-L**) are reported relative to skull length.

The direct skull length was increased in EF vs. GF mice (**Fig. 2A**), which demonstrates that commensal microbes influence the skull length. The direct skull length was similar in MPF vs. EF mice (**Fig. 2A**), which implies that commensal gut microbes do not contribute to skull length. Skull width per skull length (**Fig. 2B**), skull height per skull length (**Fig. 2C**), and nasal bone length per skull length (**Fig. 2D**) were not different in EF vs. GF mice or MPF vs. EF mice. These data support that the commensal microbiota does not influence the relative skull width, skull height, or nasal bone length in 9-week-old female C57BL/6T mice.

Cranial vault bone length analyses (**Fig. 2E-H**) demonstrated that the cranial vault length per skull length was not different in EF vs. GF mice or MPF vs. EF mice (**Fig. 2E**). The similar relative cranial vault lengths found in EF vs. GF mice and MPF vs. EF mice (**Fig. 2E**) was attributed to lack of alterations in interparietal (**Fig. 2F**) and parietal (**Fig. 2G**) bone lengths per skull length. Interestingly, the frontal bone length per skull length was increased in EF vs. GF mice and reduced in MPF vs. EF mice (**Fig. 2H**). The increased relative frontal bone length detected in EF vs. GF mice (**Fig. 2G**) infers that the commensal microbiota affects cranial vault growth and morphology. The reduced relative frontal bone length detected in MPF vs. EF mice (**Fig. 2H**) supports that commensal gut microbes play a role in commensal microbiota effects on cranial vault growth and morphology.

Cranial base bone length analyses (**Fig. 2I-L**) showed the cranial base length per skull length was decreased in EF vs. GF mice (**Fig. 2I**). The shortened relative cranial base length in EF vs. GF mice (**Fig. 2I**) was attributed to EF mice having reduced basioccipital (**Fig. 2J**), basisphenoid (**Fig. 2K**), and presphenoid (**Fig. 2L**) bone lengths per skull length. Cranial base craniometric findings in EF vs. GF mice infers that the commensal microbiota influences cranial base growth and morphology. Cranial base analyses comparing MPF vs. EF mice showed that MPF mice exhibited an increased cranial base length per skull length (**Fig. 2I**). The elongated relative cranial base length in MPF vs. EF mice (**Fig. 2I**) was due to MPF mice having an enhanced presphenoid bone length per skull length (**Fig. 2L**). Cranial base craniometric study outcomes in MPF vs. EF mice supports that commensal gut microbes contribute to commensal microbiota effects on cranial base growth and morphology.

The commensal microbiota does not affect cranial bone mineral density in 9-week-old female C57BL/6T mice.

We carried out bone mineral density (BMD) analyses in the reconstructed 3-dimensional micro-CT images of skulls to elucidate commensal microbiota effects on bone mass in the cranial vault and cranial base. Cranial vault analyses included the interparietal, parietal, and frontal bones (**Supplemental Fig. S2A-D**) and cranial base analyses included the basioccipital, basisphenoid and presphenoid bones (**Supplemental Fig. S2E-H**). Cranial vault BMD outcomes were not different in EF vs. GF mice or MPF vs. EF mice (**Supplemental Fig. S2A-D**). Furthermore, cranial base BMD outcomes were similar in EF vs. GF mice and MPF vs. EF mice (**Supplemental Fig. S2E-H**). BMD study findings support that the commensal microbiota does not critically impact bone mass accrual in the cranial vault or cranial base of 9-week-old female C57BL/6T mice.

Discussion:

This study comparing 9-week-old female C57BL/6T mice reared under defined barrier conditions, reveals the commensal microbiota plays a role in craniofacial skeletal growth and morphology. Results comparing GF mice to EF mice, showed the commensal microbiota can enlarge the gross skull length and restrict the relative cranial base length. Results comparing EF mice to MPF mice, which differ by SFB colonization status, demonstrated that MPF mice exhibited an elongated relative cranial base length. These findings support that commensal gut microbes contribute to craniofacial skeletal growth and morphology.

Comparing GF vs. EF mice demonstrated that the commensal microbiota attenuated the cranial base length, due to decreased basioccipital, basisphenoid and presphenoid lengths. Appreciating that cranial base bones form through endochondral ossification, these findings are in line with prior studies showing that the commensal microbiota regulates endochondral bone formation processes at non-oral skeletal sites.⁹⁻¹⁴ Interestingly, GF vs. EF mice exhibited an increased length in the frontal bone. The frontal bone forms through intramembranous ossification, suggesting that commensal microbiota also influences intramembranous bone formation processes.

While this initial report was centered on craniometry, future studies should evaluate suture and synchondrosis involvement. This is important because sutures and synchondroses contribute to craniofacial skeletal growth and morphology. Moreover, studies are needed to further assess commensal microbiota effects on the cranial base. The cranial base plays an extremely important role in total skull morphology as the growth site for the skull is located at the intersphenoidal synchondrosis (ISS).⁴⁸ The cranial base develops earlier than the face or the cranial vault, and has long been thought to provide patterning and instructions for the final form of the overall skull.⁴⁹ Several studies have suggested that cranial base length can predict specific malocclusions in adult life.⁵⁰ Additionally, alterations in cranial base angle have been shown to cause skeletal malocclusions.⁵¹

We investigated the 9-week-old timepoint because craniofacial skeletal growth peaks around postnatal day 60 in female C57BL/6 mice.²¹ Future investigations are needed evaluating earlier timepoints to define critical postnatal periods where the commensal microbiota contributes to craniofacial skeletal growth and morphology. We utilized micro-CT to discern commensal microbiota effects on craniometric and bone mineral density

outcomes in the postnatal craniofacial skeleton. Ongoing studies are necessary utilizing histology to delineate cellular and molecular mechanisms mediating commensal microbiota actions on growth and morphology in the craniofacial skeletal complex.

Prior work by our group and others discerned that commensal microbiota effects on non-craniofacial bone growth and morphology are influenced by mouse strain genetic determinants. Whereas the commensal microbiota impairs bone mass accrual and microarchitecture in long bones of growing C57BL/6 mice,^{9,10} the commensal microbiota promotes bone formation and longitudinal growth in long bones of growing BALB/c¹¹ and CB6F1 mice¹². Study outcomes reported herein reveal that the commensal microbiota promotes gross skull length and restricts relative cranial base length in C57BL/6 mice. Future research is necessary discern whether commensal microbiota effects on craniofacial skeletal growth and morphology differ across murine strains.

GF mice were fed LabDiet 5010 and specific-pathogen-free mice (EF, MPF mice) were fed NIH-31M diet. LabDiet 5010 and NIH-31M are standard hard pellet rodent diets, but have minor differences in composition and may differ in hardness/consistency. Knowing that administering a soft vs. hard diet can influence dentofacial growth outcomes,^{52,53} a potential study design weakness is that GF and specific-pathogen-free mice were not administered the same diet. However, all experimental groups were fed a hard diet, so minor differences in diet consistency are not expected to influence outcomes as dramatically as if the groups were fed soft vs. hard diets. Additionally, comparing EF vs. MPF mice (both fed NIH-31M) demonstrated alterations in craniofacial skeletal outcomes, which supports that commensal microbiota effects on craniofacial morphology are independent of diet. However, it is important for future studies to utilize the same diet across GF and specific-pathogen-free animal groups to eliminate diet as a potentially confounding variable.

Investigations in GF animal models have elucidated that the commensal microbiota supports normal brain development and behavior.⁵⁴⁻⁵⁷ The growth of the brain, which is housed in the skull, is a major determinant of craniofacial growth and morphology.⁵⁸⁻⁶² Therefore, commensal microbiota actions supporting normal brain development could contribute to the growth and morphology of the craniofacial skeleton through an increase in cranial capacity. This highlights the need for future research elucidating whether commensal microbiota

regulation of brain development plays a role in commensal microbiota actions on craniofacial skeletal growth and morphology.

The current investigation comparing MPF vs. EF mice, which differ by SFB colonization status, supports that commensal gut microbes play a role in the growth and morphology of the craniofacial skeleton. SFB is a commensal gut bacterium that colonizes the ileum after weaning.²⁵⁻²⁷ SFB colonization has broad innate and adaptive immunostimulatory effects, including the induction of T_H17/IL17A-mediated immunity^{27,28,63-66}. We and others have shown that SFB contributes to commensal microbiota actions on skeletal growth and maturation at non-craniofacial sites. SFB induction of T_H17/IL17A-mediated immunity promoted bone-resorbing osteoclasts and impaired trabecular bone morphology in the long bones of growing mice.^{13,14} Further, prior reports have linked SFB induction of T_H17/IL17A immunity to commensal microbiota actions in neurodevelopmental abnormalities.^{29,30} Therefore, commensal gut microbe contributions to craniofacial skeletal growth and morphology could be mediated through multifactorial effects on bone cell actions and brain development.

While SFB has been shown to colonize humans and upregulate T_H17 cell immune pathway genes⁶⁷⁻⁶⁹, *Bifidobacterium adolescentis* is another commensal gut bacterium which has been linked to the clinical induction of T_H17/IL17A-mediated immunity⁷⁰. Dietary modification^{71,72} and probiotic administration^{73,74} impact SFB colonization status, which implies that noninvasive interventions in the commensal gut microbiota could be employed to modify craniofacial skeletal growth and morphology. While randomized controlled clinical trials have shown that probiotics have protective effects on the aging skeleton and brain^{75,76}, future investigations are needed to delineate whether probiotics could be employed to direct craniofacial skeletal growth and morphology.

Our study comparing EF vs. MPF mice, which differ by a known commensal gut bacterium, supports the premise that commensal gut microbes play a role in craniofacial development. However, future research is necessary to further discern how specific microbiota communities (i.e., oral, gut) contribute to craniofacial skeletal morphology. Conventionalized animal studies, in which GF animals are associated/colonized with oral microbiota vs. gut microbiota from specific-pathogen-free mice, would delineate how different microbiota communities contribute to craniofacial skeletal growth and maturation.

Acknowledgements: Study design: JEG, NO, NEH, CMN. Study conduct: JEG, JDH, NAP, CW, CMN. Data collection: JEG, JDH, NAP, MDC. Data analysis: JEG, JDH, MDC, CMN. Data interpretation: JEG, JDH, NO, CW, NEH, CMN. Drafting manuscript: JEG, JDH, CW, CMN. All authors approved the final version of the manuscript. All authors take responsibility for the integrity of the data analysis. Graphical abstract created with BioRender.com.

References:

1. Belkaid Y, Naik S. Compartmentalized and systemic control of tissue immunity by commensals. *Nature immunology*. 2013;14(7):646-653.
2. Brestoff JR, Artis D. Commensal bacteria at the interface of host metabolism and the immune system. *Nature immunology*. 2013;14(7):676-684.
3. Thaïss CA, Zmora N, Levy M, Elinav E. The microbiome and innate immunity. *Nature*. 2016;535(7610):65-74.
4. Zheng D, Liwinski T, Elinav E. Interaction between microbiota and immunity in health and disease. *Cell Res*. 2020;30(6):492-506.
5. Sommer F, Backhed F. The gut microbiota--masters of host development and physiology. *Nature reviews Microbiology*. 2013;11(4):227-238.
6. Schroeder BO, Bäckhed F. Signals from the gut microbiota to distant organs in physiology and disease. *Nature medicine*. 2016;22(10):1079-1089.
7. Krautkramer KA, Fan J, Bäckhed F. Gut microbial metabolites as multi-kingdom intermediates. *Nature reviews Microbiology*. 2021;19(2):77-94.
8. Fan Y, Pedersen O. Gut microbiota in human metabolic health and disease. *Nat Rev Microbiol*. 2021;19(1):55-71.
9. Sjögren K, Engdahl C, Henning P, et al. The gut microbiota regulates bone mass in mice. *J Bone Miner Res*. 2012;27(6):1357-1367.
10. Novince CM, Whittow CR, Aartun JD, et al. Commensal Gut Microbiota Immunomodulatory Actions in Bone Marrow and Liver have Catabolic Effects on Skeletal Homeostasis in Health. *Scientific reports*. 2017;7(1):5747.
11. Schwarzer M, Makki K, Storelli G, et al. Lactobacillus plantarum strain maintains growth of infant mice during chronic undernutrition. *Science (New York, NY)*. 2016;351(6275):854-857.
12. Yan J, Herzog JW, Tsang K, et al. Gut microbiota induce IGF-1 and promote bone formation and growth. *Proceedings of the National Academy of Sciences of the United States of America*. 2016;113(47):E7554-e7563.
13. Hathaway-Schrader JD, Poulides NA, Carson MD, et al. Specific Commensal Bacterium Critically Regulates Gut Microbiota Osteoimmunomodulatory Actions During Normal Postpubertal Skeletal Growth and Maturation. *JBMR Plus*. 2020;4(3):e10338.
14. Tyagi AM, Darby TM, Hsu E, et al. The gut microbiota is a transmissible determinant of skeletal maturation. *eLife*. 2021;10.
15. Galea GL, Zein MR, Allen S, Francis-West P. Making and shaping endochondral and intramembranous bones. *Developmental dynamics : an official publication of the American Association of Anatomists*. 2021;250(3):414-449.
16. White HE, Goswami A, Tucker AS. The Intertwined Evolution and Development of Sutures and Cranial Morphology. *Front Cell Dev Biol*. 2021;9:653579.
17. Lacruz RS, Stringer CB, Kimbel WH, et al. The evolutionary history of the human face. *Nat Ecol Evol*. 2019;3(5):726-736.
18. Park KM, Tripathi NV, Mufarrej FA. Quality of life in patients with craniosynostosis and deformational plagiocephaly: A Systematic Review. *Int J Pediatr Otorhinolaryngol*. 2021;149:110873.
19. Kawakami M, Yamamura K. Cranial bone morphometric study among mouse strains. *BMC Evol Biol*. 2008;8:73.
20. Vora SR, Camci ED, Cox TC. Postnatal Ontogeny of the Cranial Base and Craniofacial Skeleton in Male C57BL/6J Mice: A Reference Standard for Quantitative Analysis. *Frontiers in physiology*. 2015;6:417.
21. Wei X, Thomas N, Hatch NE, Hu M, Liu F. Postnatal Craniofacial Skeletal Development of Female C57BL/6Ncrl Mice. *Front Physiol*. 2017;8:697.

22. Young DL, Schneider RA, Hu D, Helms JA. Genetic and teratogenic approaches to craniofacial development. *Critical reviews in oral biology and medicine : an official publication of the American Association of Oral Biologists*. 2000;11(3):304-317.
23. Neben CL, Merrill AE. Signaling Pathways in Craniofacial Development: Insights from Rare Skeletal Disorders. *Curr Top Dev Biol*. 2015;115:493-542.
24. Stanton E, Urata M, Chen JF, Chai Y. The clinical manifestations, molecular mechanisms and treatment of craniosynostosis. *Dis Model Mech*. 2022;15(4).
25. Klaasen HLK, J.P.; Beynen, A.C. Effects of age, strain and social hierarchy on colonization of autochthonous, segmented, filamentous bacteria in the ileum of mice. *Microecology and Therapy*. 1990b;20:17-20.
26. Snel J, Hermsen CC, Smits HJ, et al. Interactions between gut-associated lymphoid tissue and colonization levels of indigenous, segmented, filamentous bacteria in the small intestine of mice. *Canadian journal of microbiology*. 1998;44(12):1177-1182.
27. Gaboriau-Routhiau V, Rakotobe S, Lecuyer E, et al. The key role of segmented filamentous bacteria in the coordinated maturation of gut helper T cell responses. *Immunity*. 2009;31(4):677-689.
28. Ivanov, II, Atarashi K, Manel N, et al. Induction of intestinal Th17 cells by segmented filamentous bacteria. *Cell*. 2009;139(3):485-498.
29. Kim S, Kim H, Yim YS, et al. Maternal gut bacteria promote neurodevelopmental abnormalities in mouse offspring. *Nature*. 2017;549(7673):528-532.
30. Lammert CR, Frost EL, Bolte AC, et al. Cutting Edge: Critical Roles for Microbiota-Mediated Regulation of the Immune System in a Prenatal Immune Activation Model of Autism. *Journal of immunology (Baltimore, Md : 1950)*. 2018;201(3):845-850.
31. Massimi L, Bianchi F, Frassanito P, Calandrelli R, Tamburrini G, Caldarelli M. Imaging in craniosynostosis: when and what? *Childs Nerv Syst*. 2019;35(11):2055-2069.
32. Dot G, Rafflenbeul F, Arbotta M, Gajny L, Rouch P, Schouman T. Accuracy and reliability of automatic three-dimensional cephalometric landmarking. *International journal of oral and maxillofacial surgery*. 2020;49(10):1367-1378.
33. Council NR. *Guide for the Care and Use of Laboratory Animals: Eighth Edition*. Washington, DC: The National Academies Press; 2011.
34. Bacchetti De Gregoris T, Aldred N, Clare AS, Burgess JG. Improvement of phylum- and class-specific primers for real-time PCR quantification of bacterial taxa. *J Microbiol Methods*. 2011;86(3):351-356.
35. Hathaway-Schrader JD, Steinkamp HM, Chavez MB, et al. Antibiotic Perturbation of Gut Microbiota Dysregulates Osteoimmune Cross Talk in Postpubertal Skeletal Development. *Am J Pathol*. 2019;189(2):370-390.
36. Swanson BA, Carson MD, Hathaway-Schrader JD, et al. Antimicrobial-induced oral dysbiosis exacerbates naturally occurring alveolar bone loss. *FASEB journal : official publication of the Federation of American Societies for Experimental Biology*. 2021;35(11):e22015.
37. Packey CD, Shanahan MT, Manick S, et al. Molecular detection of bacterial contamination in gnotobiotic rodent units. *Gut microbes*. 2013;4(5):361-370.
38. Hathaway-Schrader JD, Aartun JD, Poulides NA, et al. Commensal oral microbiota induces osteoimmunomodulatory effects separate from systemic microbiome in mice. *JCI Insight*. 2022;7(4).
39. Livak KJ, Schmittgen TD. Analysis of relative gene expression data using real-time quantitative PCR and the 2⁻(-Delta Delta C(T)) Method. *Methods*. 2001;25(4):402-408.
40. Schmittgen TD, Livak KJ. Analyzing real-time PCR data by the comparative C(T) method. *Nature protocols*. 2008;3(6):1101-1108.
41. Hathaway-Schrader JD, Carson MD, Gerasco JE, et al. Commensal gut bacterium critically regulates alveolar bone homeostasis. *Laboratory investigation; a journal of technical methods and pathology*. 2022;102(4):363-375.

42. Liu J, Nam HK, Campbell C, Gasque KC, Millán JL, Hatch NE. Tissue-nonspecific alkaline phosphatase deficiency causes abnormal craniofacial bone development in the *Alpl(-/-)* mouse model of infantile hypophosphatasia. *Bone*. 2014;67:81-94.
43. Xu H, Lenhart SA, Chu EY, et al. Dental and craniofacial defects in the *Crtap(-/-)* mouse model of osteogenesis imperfecta type VII. *Developmental dynamics : an official publication of the American Association of Anatomists*. 2020;249(7):884-897.
44. Nam HK, Emmanouil E, Hatch NE. Deletion of the Pyrophosphate Generating Enzyme ENPP1 Rescues Craniofacial Abnormalities in the *TNAP(-/-)* Mouse Model of Hypophosphatasia and Reveals FGF23 as a Marker of Phenotype Severity. *Front Dent Med*. 2022;3.
45. Boussein ML, Boyd SK, Christiansen BA, Guldborg RE, Jepsen KJ, Müller R. Guidelines for assessment of bone microstructure in rodents using micro-computed tomography. *J Bone Miner Res*. 2010;25(7):1468-1486.
46. Liu J, Nam HK, Wang E, Hatch NE. Further analysis of the Crouzon mouse: effects of the *FGFR2(C342Y)* mutation are cranial bone-dependent. *Calcif Tissue Int*. 2013;92(5):451-466.
47. Liu J, Campbell C, Nam HK, et al. Enzyme replacement for craniofacial skeletal defects and craniosynostosis in murine hypophosphatasia. *Bone*. 2015;78:203-211.
48. Funato N. New Insights Into Cranial Synchronosis Development: A Mini Review. *Front Cell Dev Biol*. 2020;8:706.
49. Bastir M. Craniofacial levels and the morphological maturation of the human skull. *Journal of anatomy*. 2006;209:637-654.
50. Gong A, Li J, Wang Z, et al. Cranial base characteristics in anteroposterior malocclusions: A meta-analysis. *Angle Orthod*. 2016;86(4):668-680.
51. Almeida KCM, Raveli TB, Vieira CIV, Santos-Pinto AD, Raveli DB. Influence of the cranial base flexion on Class I, II and III malocclusions: a systematic review. *Dental Press J Orthod*. 2017;22(5):56-66.
52. Kiliaridis S. The Importance of Masticatory Muscle Function in Dentofacial Growth. *Seminars in orthodontics*. 2006;12(2):110-119.
53. Kono K, Tanikawa C, Murata Y, Yanagita T, Kamioka H, Yamashiro T. Three-dimensional changes in the craniofacial complex associated with soft-diet feeding. *Eur J Orthod*. 2020;42(5):509-516.
54. Diaz Hejtz R, Wang S, Anuar F, et al. Normal gut microbiota modulates brain development and behavior. *Proceedings of the National Academy of Sciences of the United States of America*. 2011;108(7):3047-3052.
55. Hoban AE, Stilling RM, Ryan FJ, et al. Regulation of prefrontal cortex myelination by the microbiota. *Translational psychiatry*. 2016;6(4):e774.
56. Lu J, Synowiec S, Lu L, et al. Microbiota influence the development of the brain and behaviors in C57BL/6J mice. *PloS one*. 2018;13(8):e0201829.
57. Ahmed S, Travis SD, Díaz-Bahamonde FV, et al. Early Influences of Microbiota on White Matter Development in Germ-Free Piglets. *Front Cell Neurosci*. 2021;15:807170.
58. Moss ML, Young RW. A functional approach to craniology. *American Journal of Physical Anthropology*. 1960;18(4):281-292.
59. Lieberman DE, Pearson OM, Mowbray KM. Basicranial influence on overall cranial shape. *Journal of human evolution*. 2000;38(2):291-315.
60. Hallgrímsson B, Lieberman DE. Mouse models and the evolutionary developmental biology of the skull. *Integr Comp Biol*. 2008;48(3):373-384.
61. Marcucio RS, Young NM, Hu D, Hallgrímsson B. Mechanisms that underlie co-variation of the brain and face. *Genesis*. 2011;49(4):177-189.
62. Adameyko I, Fried K. The Nervous System Orchestrates and Integrates Craniofacial Development: A Review. *Frontiers in physiology*. 2016;7:49.
63. Goto Y, Panea C, Nakato G, et al. Segmented filamentous bacteria antigens presented by intestinal dendritic cells drive mucosal Th17 cell differentiation. *Immunity*. 2014;40(4):594-607.

64. Lecuyer E, Rakotobe S, Lengline-Garnier H, et al. Segmented filamentous bacterium uses secondary and tertiary lymphoid tissues to induce gut IgA and specific T helper 17 cell responses. *Immunity*. 2014;40(4):608-620.
65. Panea C, Farkas AM, Goto Y, et al. Intestinal Monocyte-Derived Macrophages Control Commensal-Specific Th17 Responses. *Cell reports*. 2015;12(8):1314-1324.
66. Flannigan KL, Ngo VL, Geem D, et al. IL-17A-mediated neutrophil recruitment limits expansion of segmented filamentous bacteria. *Mucosal immunology*. 2017;10(3):673-684.
67. Yin Y, Wang Y, Zhu L, et al. Comparative analysis of the distribution of segmented filamentous bacteria in humans, mice and chickens. *The ISME journal*. 2013;7(3):615-621.
68. Chen B, Chen H, Shu X, et al. Presence of Segmented Filamentous Bacteria in Human Children and Its Potential Role in the Modulation of Human Gut Immunity. *Frontiers in microbiology*. 2018;9:1403.
69. Chen H, Wang L, Wang X, Wang X, Liu H, Yin Y. Distribution and Strain Diversity of Immunoregulating Segmented Filamentous Bacteria in Human Intestinal Lavage Samples. *Microbial ecology*. 2020;79(4):1021-1033.
70. Tan TG, Sefik E, Geva-Zatorsky N, et al. Identifying species of symbiont bacteria from the human gut that, alone, can induce intestinal Th17 cells in mice. *Proceedings of the National Academy of Sciences of the United States of America*. 2016;113(50):E8141-e8150.
71. Koopman JP, van den Brink ME, Scholten PM. Further studies with the segmented filamentous intestinal bacteria of mice; effects of physical and chemical factors on survival and the effects of milk diet, para-aminobenzoic acid and mouse strain on colonization. *Zeitschrift für Versuchstierkunde*. 1988;31(6):270-275.
72. Koopman JP, van den Brink ME, Scholten PM, et al. The influence of stress and cheese-whey on intestinal parameters in mice. *The Veterinary quarterly*. 1989;11(1):24-29.
73. Fuentes S, Egert M, Jimenez-Valera M, Monteoliva-Sanchez M, Ruiz-Bravo A, Smidt H. A strain of *Lactobacillus plantarum* affects segmented filamentous bacteria in the intestine of immunosuppressed mice. *FEMS microbiology ecology*. 2008;63(1):65-72.
74. Liao N, Yin Y, Sun G, et al. Colonization and distribution of segmented filamentous bacteria (SFB) in chicken gastrointestinal tract and their relationship with host immunity. *FEMS microbiology ecology*. 2012;81(2):395-406.
75. Nilsson AG, Sundh D, Bäckhed F, Lorentzon M. *Lactobacillus reuteri* reduces bone loss in older women with low bone mineral density: a randomized, placebo-controlled, double-blind, clinical trial. *Journal of internal medicine*. 2018;284(3):307-317.
76. Kim CS, Cha L, Sim M, et al. Probiotic Supplementation Improves Cognitive Function and Mood with Changes in Gut Microbiota in Community-Dwelling Older Adults: A Randomized, Double-Blind, Placebo-Controlled, Multicenter Trial. *The journals of gerontology Series A, Biological sciences and medical sciences*. 2021;76(1):32-40.

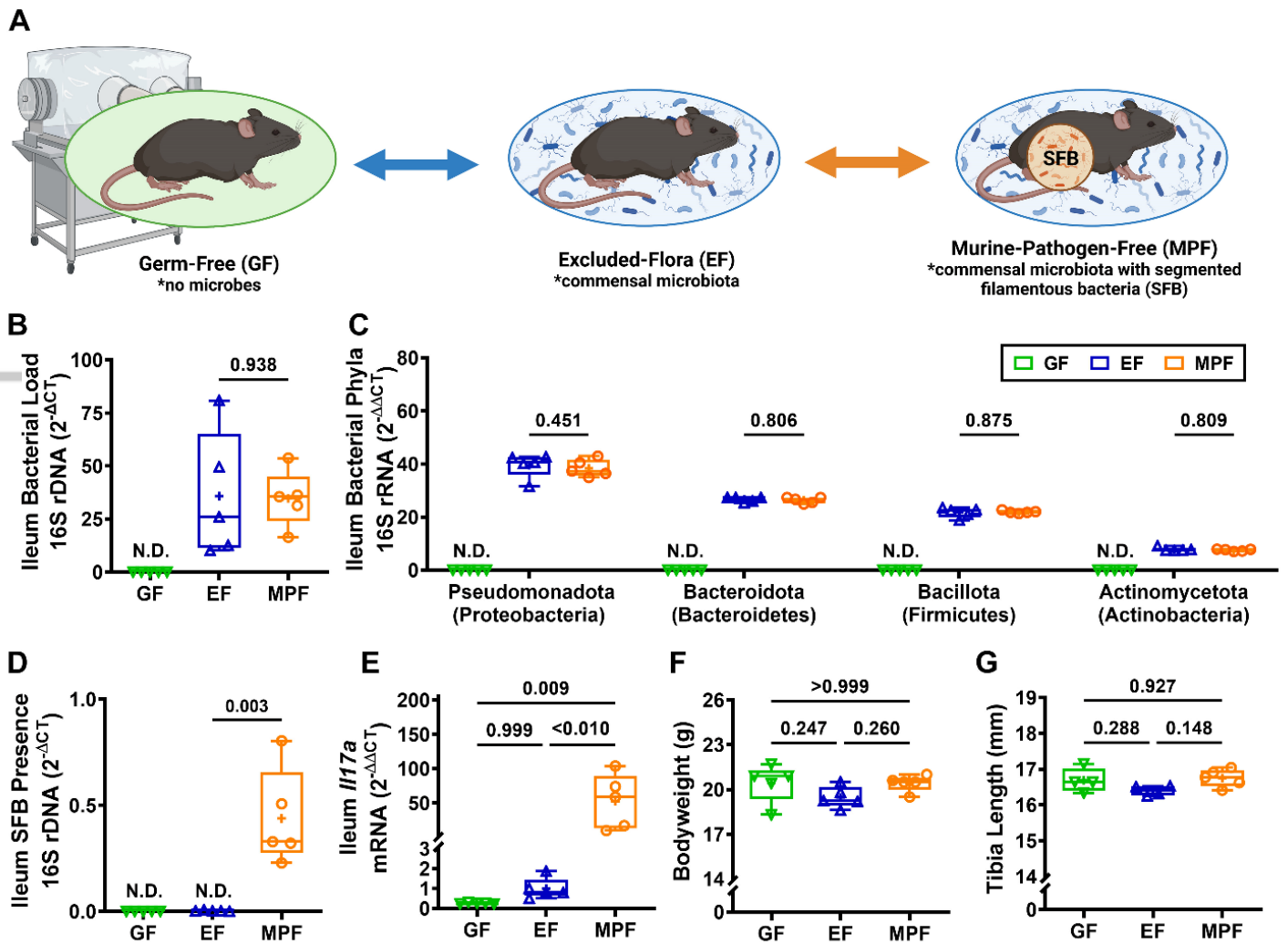


Figure 1. The commensal microbiota does not alter somatic growth in 9-week-old female C57BL/6T mice. (A) Female C57BL/6T germ-free (GF) mice (no microbes), EF mice (commensal microbiota), and MPF mice (commensal microbiota with segmented filamentous bacteria; SFB) were euthanized at age 9-weeks; specimens were isolated for analyses. (A) Schematic of study design. (B-D) qRT-PCR 16S rDNA analysis of ileum contents (n=5/group) evaluating (B) bacterial load (C) phyla, and (D) SFB presence. (B) Bacterial load determined by normalizing the Universal 16S gene to a bacterial DNA standard; quantification via the $2^{-\Delta CT}$ method. (C) Phylum outcomes determined by normalizing phylum 16S genes to the Universal 16S gene; quantification by the $2^{-\Delta\Delta CT}$ method. (D) SFB presence determined by normalizing the SFB 16S gene to a bacterial DNA standard; quantification via the $2^{-\Delta CT}$ method. (E) qRT-PCR mRNA analysis of *Ili7a* in ileum (n=5/group); relative quantification of mRNA was performed via the $2^{-\Delta\Delta CT}$ method. (F) Bodyweight analysis (n=5/group). (G) Tibia length analysis (n=4-5/group). (B-D) Unpaired two-tailed t-test (P-value < 0.05) was performed comparing 16S rDNA analysis outcomes in EF vs. MPF mice. (E-F) One-way ANOVA (alpha = 0.05) with Tukey post-hoc test (P-value < 0.05) was carried out comparing outcomes in GF, EF, and MPF mice.

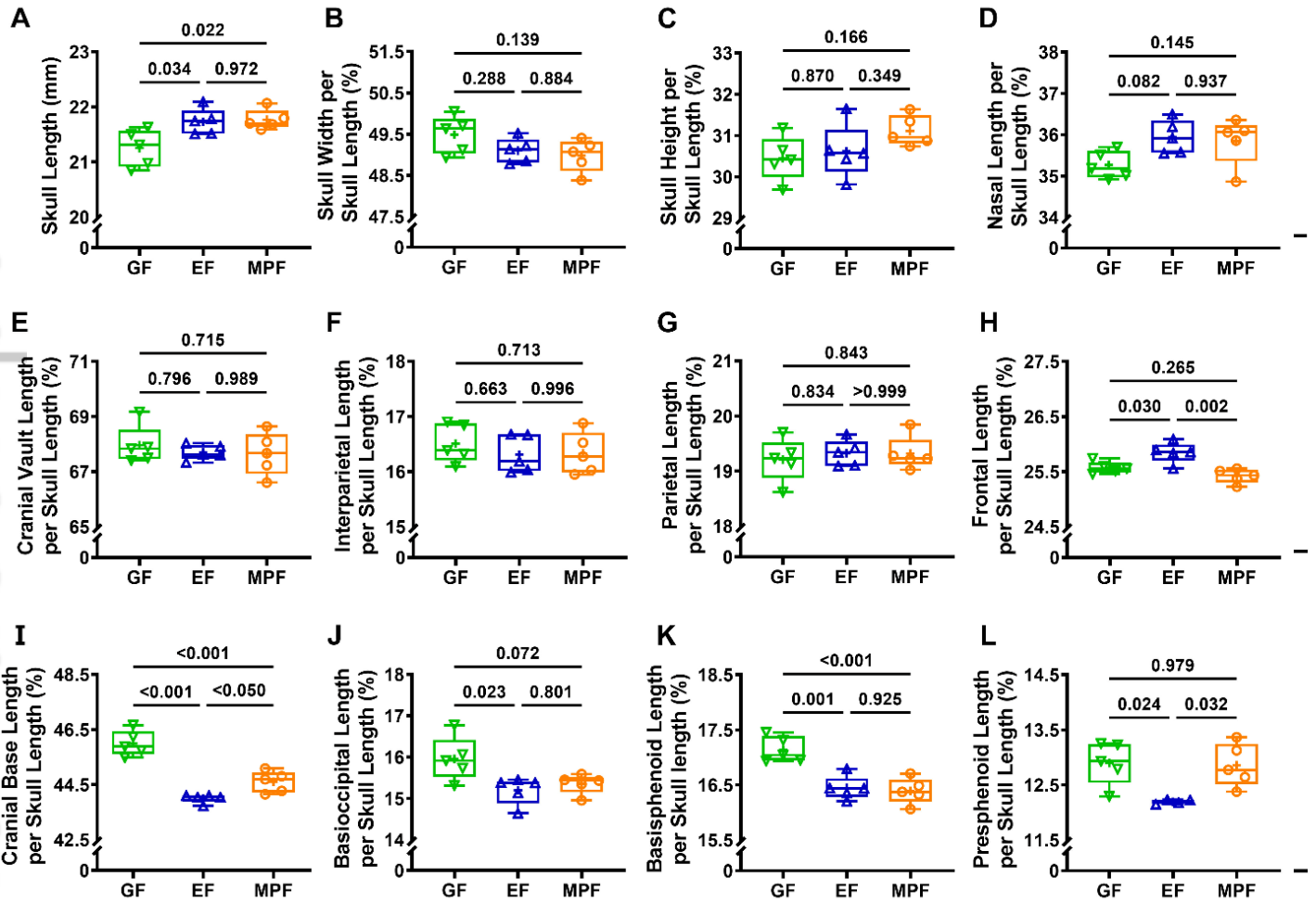
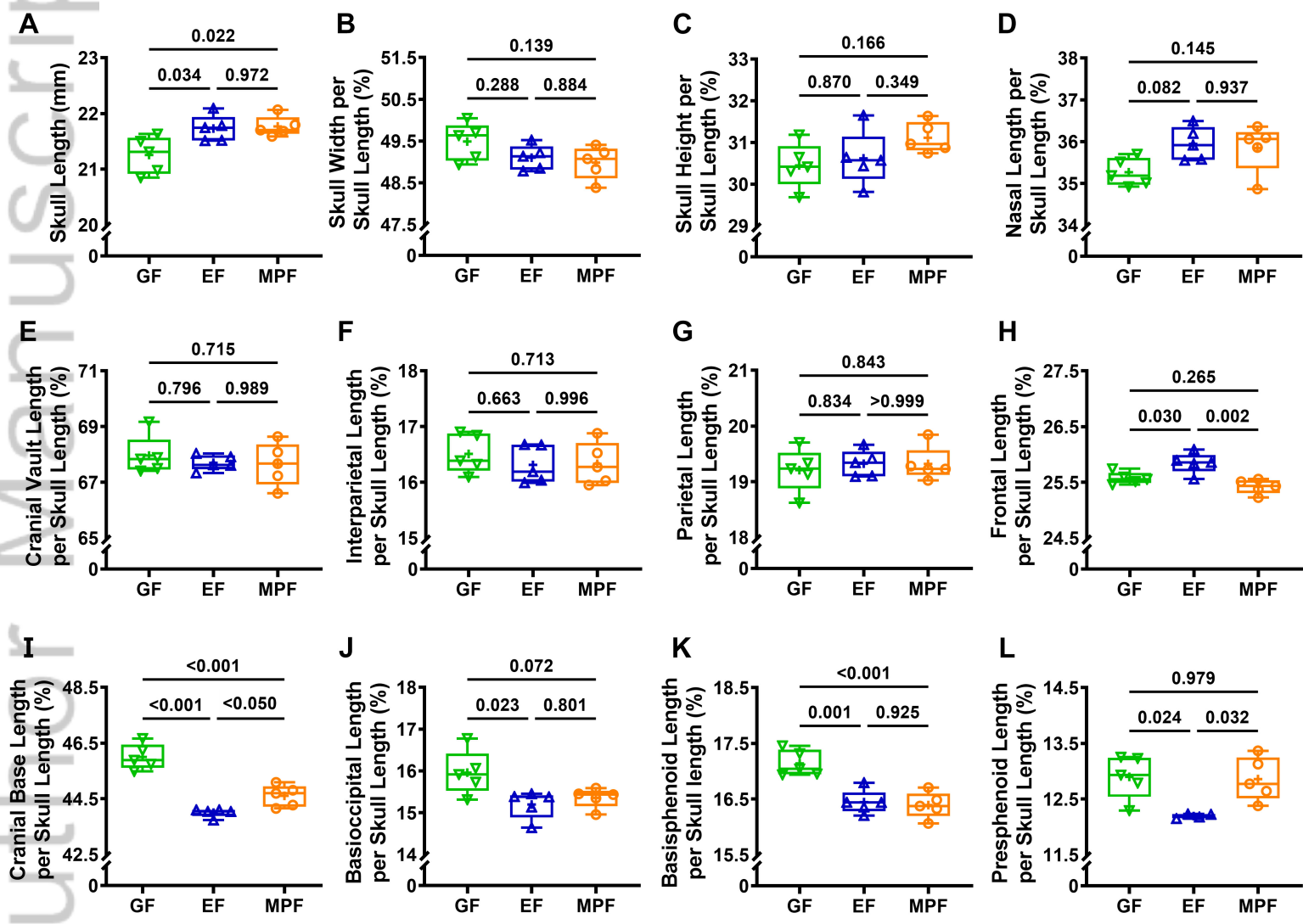
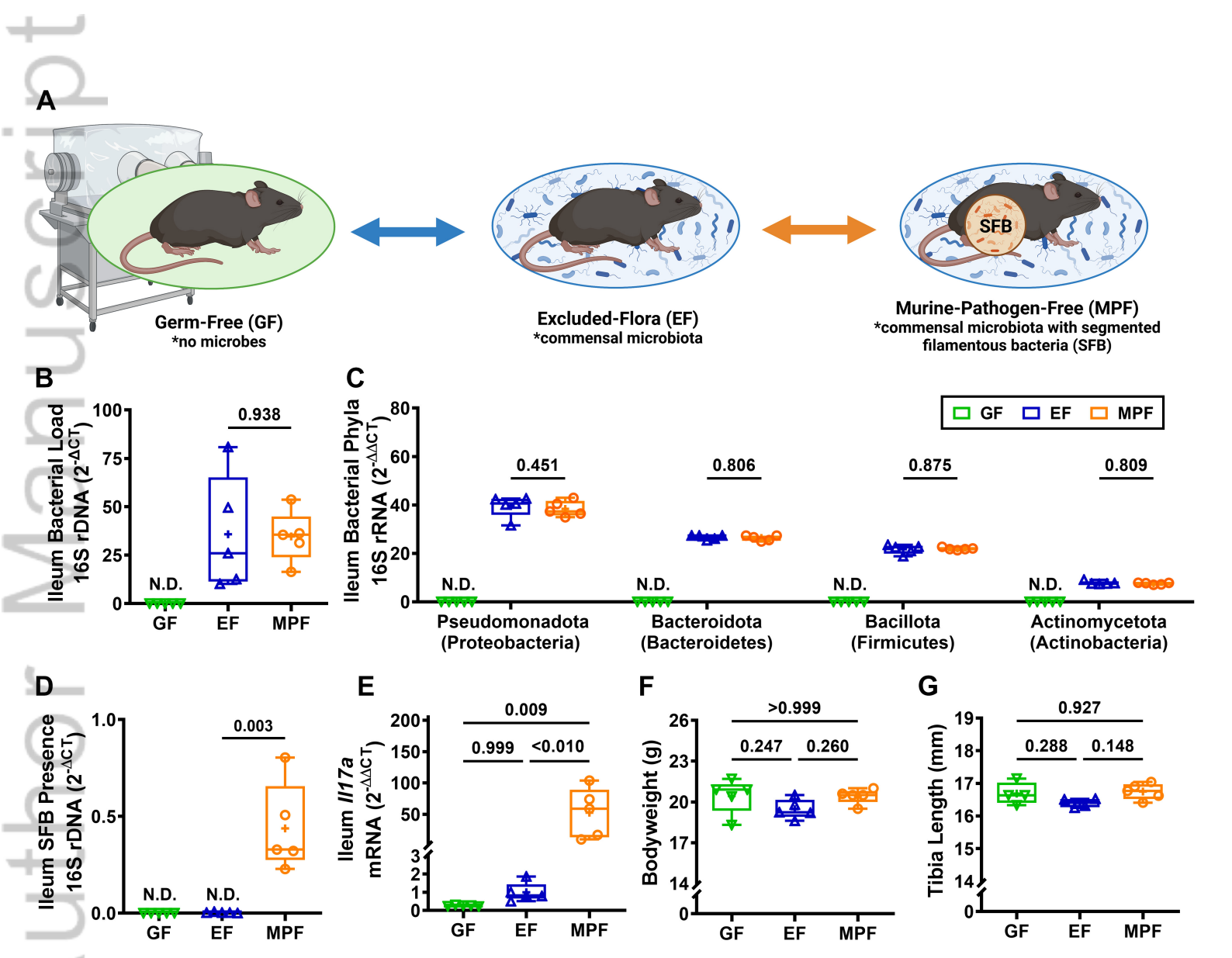


Figure 2. The commensal microbiota impacts craniofacial skeletal morphology in 9-week-old female C57BL/6T mice. Female C57BL/6T germ-free (GF) mice (no microbes), EF mice (commensal microbiota), and MPF (MPF) mice (commensal microbiota with segmented filamentous bacteria; SFB) were euthanized at age 9-weeks; skulls were isolated for analyses (n=5/group). Craniometric measurements were performed using micro-CT 3D reconstructions of the skull and standard craniometric landmarks (**Figure S1**). skull length (**A**); skull width (**B**); skull height (**C**); nasal length per skull length (**D**); cranial vault length per skull length (**E**); interparietal bone length per skull length (**F**); parietal bone length per skull length (**G**); frontal bone length per skull length (**H**); cranial base length per skull length (**I**); basioccipital bone length per skull length (**J**); basisphenoid bone length per skull length (**K**); presphenoid bone length per skull length (**L**). One-way ANOVA ($\alpha = 0.05$) with Tukey post-hoc test ($P\text{-value} < 0.05$) was carried out comparing outcomes in GF, EF, and MPF mice.



JBM4_10775_figure 2_rev (1).tif



JBM4_10775_Figure 1_rev (1).tif

Graphical Abstract Description: Comparing germ-free mice (no microbes) to excluded-flora mice (commensal microbiota), showed the commensal microbiota influences craniofacial skeletal growth and morphology (*blue arrows denote commensal microbiota-induced changes). Comparing excluded-flora mice (commensal microbiota) to murine-pathogen-free mice (commensal microbiota with segmented filamentous bacteria; SFB), revealed that specific commensal gut microbes contribute to craniofacial skeletal growth and morphology (*orange arrows denote SFB-induced changes).

Commensal Microbiota Contributions to Craniofacial Skeletal Morphology

